Faraday Discussions

Cite this: *Faraday Discuss.*, 2014, **176**, 125

PAPER

Activity–stability relationship in the surface electrochemistry of the oxygen evolution reaction

Seo Hyoung Chang, Justin G. Connell, Nemanja Danilovic, Ram Subbaraman, Kee-Chul Chang, Vojislav R. Stamenkovic and Nenad M. Markovic*

Received 18th June 2014, Accepted 25th July 2014
DOI: 10.1039/c4fd00134f

Understanding the functional links between the stability and reactivity of oxide materials during the oxygen evolution reaction (OER) is one key to enabling a vibrant hydrogen economy capable of competing with fossil fuel-based technologies. In this work, by focusing on the surface chemistry of monometallic Ru oxide in acidic and alkaline environments, we found that the kinetics of the OER are almost entirely controlled by the stability of the Ru surface atoms. The same activity–stability relationship was found for more complex, polycrystalline and single-crystalline $SrRuO_3$ thin films in alkaline solutions. We propose that the electrochemical transformation of either water (acidic solutions) or hydroxyl ions (alkaline solutions) to di-oxygen molecules takes place at defect sites that are inherently present on every electrode surface. During the OER, surface defects are also created by the corrosion of the Ru ions. The dissolution is triggered by the potential-dependent change in the valence state (n) of Ru: from stable but inactive Ru^{4+} to unstable but active $Ru^{n>4+}$. We conclude that if the oxide is stable then it is completely inactive for the OER. A practical consequence is that the best materials for the OER should balance stability and activity in such a way that the dissolution rate of the oxide is neither too fast nor too slow.

Introduction

The development of true energy security requires the expansion of renewable energy sources as viable alternatives to fossil fuel-based technologies. In many of the concepts currently under consideration, hydrogen is the key energy carrier and, despite several hurdles that still need to be overcome, it seems that hydrogen is indeed the most likely fuel of the future.[1–3] Interestingly, the realization of a viable hydrogen economy is closely tied to developing greater understanding of the factors that influence the efficiency of di-oxygen electrochemistry, in

Materials Science Division, Argonne National Laboratory, 9700 S Cass Ave, Argonne, IL 60439, USA. E-mail: nmmarkovic@anl.gov

particular, designing active and stable anode materials for the oxygen evolution reaction (OER: $2H_2O \leftrightarrow O_2 + 4H^+ + 4e^-$ for acid and $4OH^- \leftrightarrow O_2 + 2H_2O + 4e^-$ for alkaline).[1,4] The OER generally suffers from significant kinetic limitations, so the reaction takes place well above the reversible potential for the OER of 1.23 V.[1] The kinetics of the OER have, for the most part, been closely tied to the concept of the volcano plot, which generally expresses the rate of the OER as a function of more fundamental properties of the oxide materials, known as descriptors.[4–7] These analyses showed that the interaction between the substrate and the reactants, intermediates, and the products has to be optimized for the reaction to proceed efficiently.[8–11] Although concepts resulting from volcano plot analyses have led to the establishment of important catalytic trends, many fundamental questions still remain open. One key question is what relationship exists between the kinetics of the OER and the stability of the oxide materials. The lack of understanding of such stability–activity relationship derives mainly from the fact that research directed at the development of anode materials for the OER has been strongly "activity-centric", while almost completely ignoring the stability of the active components *during* the OER.

Here, we show that this disparity in focus has masked the inherently close ties that exist between the stability and activity of monometallic and complex oxide Ru-based catalysts. By studying the stability–activity relationship of well-characterized Ru oxide and $SrRuO_3$ single crystal thin films in aqueous environments, we demonstrate that there is a fundamental link between the stability of catalysts and their reactivity in the OER. This trend is observed for Ru metal electrodes in both acidic and alkaline electrolytes, indicating that the stability–activity relationship is independent of the specific ionic/molecular species mediating the OER (*i.e.* OH^- *vs.* H_2O). We found that the degree of stability is always inversely proportional to the activity, and that stable surfaces are, in fact, not reactive.

Results and discussion

Relationship between stability of Ru oxide and reactivity for the OER

We begin by summarizing cyclic voltammograms (CVs) for a polycrystalline Ru electrode in both acidic and alkaline media. Inspection of Fig. 1a reveals that, independent of the pH of the solution, the adsorption of the oxygenated species on Ru occurs across the entire voltage window from the hydrogen evolution to the oxygen evolution potential regions. We note that the as-deposited polycrystalline Ru electrode surfaces are immediately converted to Ru oxide during the OER, and that this surface "hydrous oxide", formed by water electrooxidation at high anodic potentials, is distinct from a thermally-grown oxide in that it is amorphous, full of defects and contains hydroxyl species.[12] In order to understand how the electrode potential may affect the stability of the electrode surface before and during the OER, we measured the oxidation state of Ru using *in situ* X-ray absorption near edge structure (XANES) analysis. The inset in Fig. 1b shows typical XANES spectra recorded at 0.05 V, 1.25 V, and 1.45 V. The XANES spectra of Ru between 0.05 V and 0.8 V show no difference compared with standard Ru metal spectra, *e.g.*, Ru electrodes are in the $n = 0$ valence state. This indicates that reversible adsorption of hydroxyl species at this potential has no significant effect on the oxidation state of Ru. In acidic media, above 0.8 V the valence state systematically changes from $n = 0$ to $n = 3+$ between $0.8 < E < 1.0$ V, to mixtures of $n = 3+$ and $n = 4+$ between $1.0 < E$

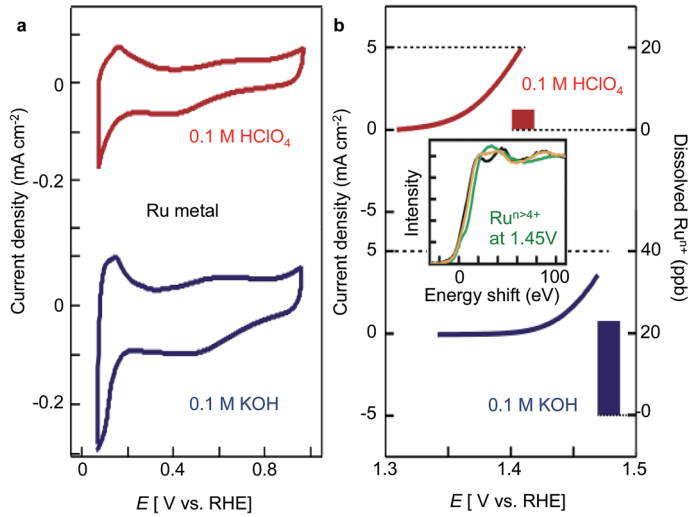

Fig. 1 (a) Cyclic voltammograms (CV) of Ru metal catalysts in acid (red line, 0.1 M $HClO_4$) and alkaline (blue line, 0.1 M KOH) electrolytes. (b) Activity of the oxygen evolution reaction (OER) (solid line) and Ru dissolution monitored by inductively-coupled plasma (ICP) measurements at a constant current density of 5 mA cm^{-2} (solid bars). The inset shows *in situ* XANES spectra at the potentials; 0.05 V (black), 1.25 V (yellow), and 1.45 V (green). The potentials are given *versus* the reversible hydrogen electrode (RHE).

< 1.3 V, and to $n > 4+$ for $E > 1.4$ V. Very similar changes in the valence state are also observed in the alkaline solution, with the only difference being that the change from $n = 4+$ to $n > 4+$ is shifted towards more positive potentials (1.47 V and above).

The relationships between the valence state of Ru, stability and reactivity were explored by monitoring the electrode potential-dependent Ru dissolution before and during the OER, by combining XANES with inductively-coupled plasma (ICP) measurements. As shown in Fig. 1b, the onset potential of the OER in acid is lower than that in alkaline solution, at the same disk current density of 1 mA cm^{-2}, implying that the OER is more active in acid than in alkaline solution. In addition, the dissolution of Ru in both electrolytes as measured by ICP is mirrored in the XANES data by a transition in the Ru valence state from $n = 4+$ to $n > 4+$, signaling that Ru dissolution is always triggered by the appearance of higher Ru oxidation states. We note that the ICP measurements were carried out at a constant current density of 5 mA cm^{-2}, as the difference in activity between the acid and alkaline solutions is large enough that it was very difficult to probe dissolution at the same overpotential. These observations highlight how potential-dependent variations in the oxidation state of the near-surface oxide can affect the stability of the surface atoms, as well as show that reactivity is intrinsically linked to the stability of these oxide materials.

Relationship between stability of Ru and $SrRuO_{3-x}$ polycrystalline electrodes and reactivity for the OER

Having established the functional links between Ru stability and activity for the OER, we investigated whether the same trends hold for Ru-based complex oxide materials such as $SrRuO_3$. To explore the role of Ru in these two different oxides, polycrystalline Ru and $SrRuO_{3-x}$ thin films (estimated thickness 10–30 nm) were

sputter-deposited (AJA International, Inc.) at 200 °C onto conductive glassy carbon substrates. We verified that both samples showed characteristic Ru spectra in XANES, and that they exhibited high conductance using a probe station.[13] Polarization curves, shown in Fig. 2, show that the $SrRuO_{3-x}$ thin films are less electrocatalytically active for the OER than the monometallic Ru oxide. ICP measurements (Fig. 2, inset) were carried out for both samples at the same overpotential (rather than at constant current density as in Fig. 1b) in order to quantitatively compare the concentration of dissolved Ru during the OER. These data clearly show that the Ru concentration found in the electrolyte is much higher for the Ru oxide than for $SrRuO_{3-x}$, confirming that activity is controlled by the stability of the Ru active sites. Note that for the ICP measurements, the electrolyte was sampled at the end of the positive potentiodynamic OER sweep. Given that the same behavior is observed for experiments performed at a constant voltage (0.1 V from the reversible potential),[12] it is reasonable to suggest that the higher rates of Ru dissolution from monometallic oxides are associated with the lower stability of Ru oxide. In turn, dissolution is accompanied by the simultaneous formation of defect sites, which result in the higher reactivity of Ru surfaces relative to $SrRuO_{3-x}$. These results clearly show that there is a strong relationship between the activity and stability of the electrode surface, as well as that the density of the surface defects, present both intrinsically on the as-prepared surfaces and created during Ru dissolution, play a key role in determining the reactivity of the oxide materials. Nevertheless, the polycrystalline nature of the electrodes precludes a more precise understanding of the relationship between the nature and density of surface defects and the reactivity of the Ru-based oxides. In order to more precisely investigate this relationship and to establish fundamental links between activity and stability, it is necessary to synthesize oxide samples with highly controlled surface structures.

Relationship between stability of the $SrRuO_3$ single crystal films and reactivity for the OER

Toward this end, we synthesized single-crystalline $SrRuO_3$ (SRO) thin films for use as a model system to investigate the role of surface structure on electrocatalytic

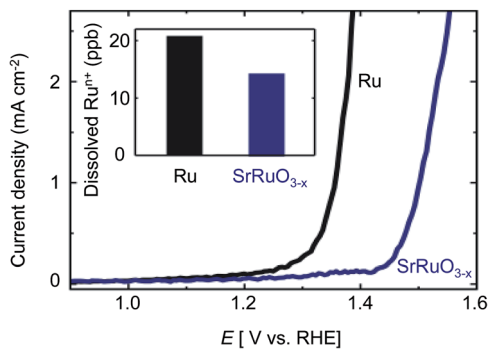

Fig. 2 Activity and stability of polycrystalline ruthenium-based catalysts for the OER, Ru (black) and $SrRuO_{3-x}$ (blue), on glassy carbon substrates. The inset shows the amount of dissolved Ru in the samples after OER processes, using ICP measurements within the same potential range.

activity and stability during cycling. Single crystal SRO is an ideal model system to study due to its high conductivity (~5000 Ω^{-1} m^{-1}) and its ability to readily grow high-quality thin films where it is possible to change the surface termination, as shown in Fig. 3a–c. For example, films grown along the (001) direction (Fig. 3a) are non-polar in the ionic limit, meaning that there is no net surface charge on the exposed surface layer. In contrast, films grown along the (110) and (111) directions (Fig. 3b and c) are polar, with alternating $(SrRuO)^{4+}/(O_2)^{4-}$ and $(Ru)^{4+}/(SrO_3)^{4-}$ layers, respectively. As a result, by simply varying the growth direction of the thin film it is possible to investigate the effects of the presence of surface energy differences, due to any residual polarity or under-coordinated polar surfaces, on the electrochemical activity and stability.[14]

The films were grown using radio-frequency (RF) magnetron sputter deposition (AJA International, Inc.), and conductive, 0.5 wt% Nb-doped $SrTiO_3$ (STO) substrates were used to improve the overall sample conductance. The SRO films exhibit a perovskite (ABO_3) crystal structure, with Ru ions surrounded by six oxygen ions (Fig. 3a). The lattice parameter of the SRO film is very close to that of the STO substrate (~0.64% with compressive strain), enabling the growth of high-quality, epitaxial thin films.[15,16] By controlling the orientation of the STO substrate, *e.g.* (001), (110), or (111), the growth direction and resulting surface structure of the SRO films were likewise able to be modified, and the CV measurements of the as-grown SRO (001), (110) and (111) thin films (Fig. 3d) show that the pseudocapacitance increases as (001) < (110) < (111).

Despite the choice of conductive, Nb-doped STO substrates, we found that the activity of the SRO films was hindered by the low conductance of the substrate. Note that conductivity of SRO is approximately 100 times higher than that of 0.5 wt% Nb:STO at room temperature. The current density–voltage characteristics of our SRO samples were measured through the bottom of the substrate using a conventional two-probe measurement system (Keithley 237 Source Measure Unit), and revealed nonlinear *I–V* behavior (Fig. 3e). Such nonlinear behavior is

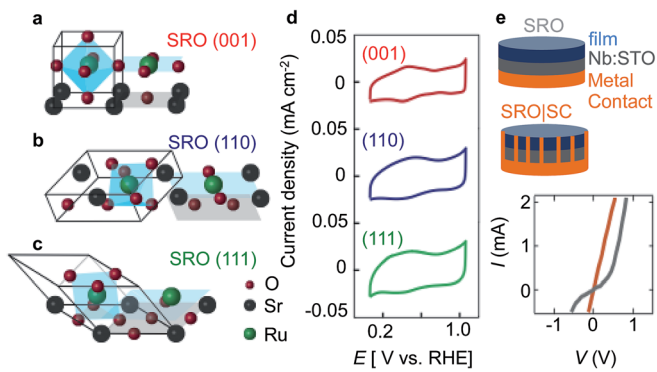

Fig. 3 (a–c) Schematics of the $SrRuO_3$ (SRO) films with different crystal structures grown on Nb-doped $SrTiO_3$ (STO) substrates (001), (110), and (111) respectively. (d) CVs of the SRO (001), (110), and (111) films. (e) Schematics and current–voltage (*I–V*) characteristics for the SRO/Nb:STO interface. Samples with and without a side contact (SC) between the SRO top surface and the backside of the substrate are denoted by SRO|SC (red line) and SRO (grey line), respectively.

indicative of high resistance as a result of a Schottky barrier at one of two locations: (1) the metal contact and Nb:STO substrate or (2) the SRO film and the Nb:STO substrate. The possibility of a Schottky barrier at the substrate–contact interface was eliminated by depositing a layer of Ti/Pt underneath the Ti metal contact, resulting in the formation of an Ohmic contact between Ti and STO. To avoid the formation of a contact between the SRO top surface and the backside of the substrate, we enclosed the perimeter of the samples with Kapton tape after mounting onto the sample chuck, prior to the start of the Ti/Pt room temperature deposition, and X-ray photoelectron spectroscopy (XPS) showed no indication of Ti or Pt contamination on the SRO surface after contact deposition. However, nonlinear *I–V* behavior was still observed even after ensuring Ohmic contact between the metal and substrate, suggesting that there is a Schottky barrier between the SRO and Nb:STO. Indeed, this is unsurprising given that there is a large difference between the work function of SRO (5.2 eV) and the electron affinity of the n-type semiconducting Nb:STO substrate (3.9 eV).[17] Unfortunately, it is very challenging to identify an interlayer material that can provide an Ohmic contact between SRO and STO while still enabling the growth of high-quality SRO thin films.

To circumvent this issue and verify the intrinsic activity of the SRO samples, a method was developed to directly contact the SRO thin film and enable analysis of the stability and activity of SRO. We prepared two sets of samples to compare the electrical behavior and verify the formation of an Ohmic contact: SRO with a metallic side connection (SRO|SC) and SRO without a side connection (SRO). Using these two samples, we observed that the presence of a metal side contact resulted in the formation of an Ohmic contact to the SRO thin film (Fig. 3e); however, the only difference in catalytic behavior observed between the two samples was that the kinetics of dissolution of the SRO thin film were slower on the SRO sample without a SC than for the SRO|SC sample. As a result, we made use of the slower kinetics of dissolution on the SRO samples without SC to enable more precise measurements of the kinetics of the OER, and investigate the relationship between the activity and stability of SRO. Detailed investigations of the stability of the SRO (001) films have been described elsewhere;[13] however, the results below provide new insight into the electrochemical behavior of this material and confirm the initial findings.

Polarization curves (Fig. 4a) were measured to examine the OER activity and stability of the SRO thin films on Nb:STO (001) in 0.1 M KOH electrolyte. The thin films were repeatedly cycled from 0 V to 1.95 V in order to trigger the OER and monitor changes in activity with cycling. We observed that the activity of the SRO film decreased gradually with the number of voltage cycles, with the OER current density decreasing by a factor of seven over 25 cycles. Atomic force microscopy (AFM) measurements (Fig. 4b) acquired before and after cycling indicate that the surface is initially terraced, with few intrinsic defects, but after cycling it becomes substantially roughened and exhibits many nano-sized islands that are randomly distributed on the surface. *In situ* X-ray scattering and XANES experiments confirmed that the SRO thin film was completely degraded after cycling, and revealed that the Ru oxidation state changes from $n = 4+$ to $n > 4+$ when holding at 1.45 V (ref. 13). Given these results, it is likely that the decrease in the OER current density after cycling originates from the dissolution of Ru ions after the formation of Ru active sites with $n > 4+$, which is consistent with our observations above on

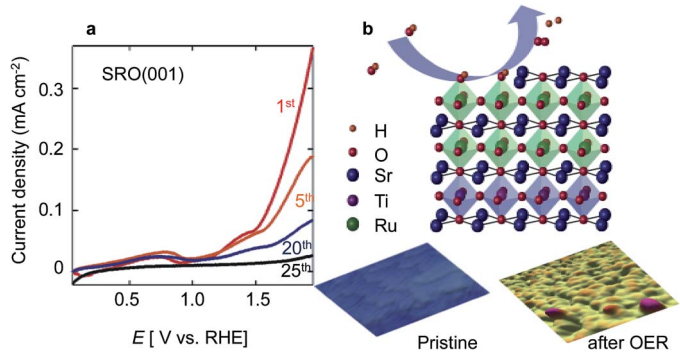

Fig. 4 (a) Successive changes in the current density on SRO (001) for the OER after various numbers of potential cycles. (b) Schematics of the model system and the OER process. AFM topography of the atomically flat SRO thin film surface ($1 \times 1\ \mu m^2$) with step terraces prior to cycling. After the OER, the film surfaces became rough, with RMS values increasing from 0.25 nm to 2.4 nm.

Ru metal (Fig. 1b). Note that the Ru active sites with an oxidation state of $n > 4+$ are easily dissolved and therefore do not remain at the surface indefinitely to serve as active sites. As our SRO films are very thin (10–30 nm), dissolution has a large impact on the observed activity due to the finite number of Ru atoms present in the film, relative to a bulk Ru sample. In fact, thicker polycrystalline SRO thin films (>100 nm) are more stable, with no difference in activity observed between the first and second potential sweep. As with the Ru metal, single crystal SRO surfaces are unstable and the OER on SRO is always accompanied by the dissolution of Ru cations.

The activity and stability for the OER in alkaline environments on Ru-based oxides – Ru, SRO polycrystalline films and SRO (001), (110) and (111) single crystalline films – are summarized in Fig. 5. This information provides insights into the material properties that influence the stability and activity of metal oxide surfaces during the OER – in particular, surface structure (polycrystalline *vs.* single crystal) and surface orientation. We observe that the activity of polycrystalline Ru metal is higher than that of polycrystalline SRO, whereas the stability of polycrystalline SRO is higher than that of Ru metal. A similar inverse relationship between activity and stability is observed for single crystalline SRO thin films, with the activity increasing in the order (001) < (110) < (111) and the stability increasing in the opposite order. Overall the activity of the crystalline SRO is lower than that of the polycrystalline samples, which is consistent with the expectation that single crystalline surfaces have a lower concentration of surface defects relative to polycrystalline samples.

Given these trends, we suggest that the density of the defects on the surface plays a significant role in determining the observed relationship between activity and stability. Interestingly, similar trends have recently been observed on other noble metal surfaces such as Au, Pt and Ir (ref. 12) – suggesting that the inverse relationship between activity and stability is a general phenomenon for electrocatalysts for the OER. In ref. 12, the role of the defects was probed by comparing activity *vs.* stability on the same materials with different surface structures. It was found that less defective single crystals of Ru are more stable, but less active, than

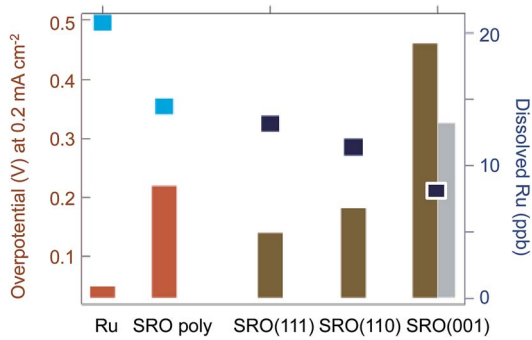

Fig. 5 Functional links between the stability and activity of Ru-based electrocatalysts (Ru, $SrRuO_{3-x}$ polycrystalline film and SRO single crystalline films from ref. 13) for the OER. The activity (bars) is measured by the OER overpotential at 0.2 mA cm^{-2}. [Note that data for SRO (001) at 0.2 mA cm^{-2} are an extrapolation from ref. 13 and the grey bar is the overpotential of SRO (001) at 0.1 mA cm^{-2}.] The stability (solid dots) is measured by the dissolved Ru species in the electrolyte (0.1 M KOH).

the polycrystalline Ru electrodes. Given that the same was observed for Ir in that work, we conclude that the inverse activity–stability relationship observed in this work is valid for many other oxide systems. Furthermore, *in situ* XANES measurements on all samples indicate that the onset of Ru dissolution into the electrolyte is accompanied by a change in the Ru oxidation state from $n = 4+$ to $n > 4+$, suggesting that the activity of Ru-based materials for the OER is dictated by the transition in Ru oxidation state. We propose that, in fact, the "active sites" for Ru-based electrocatalysts are locations on the electrode surface with Ru atoms in oxidation states greater than 4+.

In conclusion, the catalytic trends established thus far on high surface area materials should be revisited, and when possible, investigated on well-characterized single crystal surfaces. Targeted, detailed studies are necessary in order to unravel the relationship between stability and activity of oxide surfaces in electrochemical environments. Finally, although this work has focused on Ru-based materials, the fundamental and practical implications of the relationship between stability and activity likely extend well beyond this particular system, and will be extremely helpful in the design of new oxide materials that can serve as both active *and* stable electrocatalysts in aqueous environments and organic solutions.

Experimental

Thin film growth

The polycrystalline Ru and $SrRuO_{3-x}$ samples (5–200 nm) were grown at 200 °C, at a total pressure of 15 mTorr, using an RF-sputtering system on conducting glassy carbon substrates. Epitaxial $SrRuO_3$ films (10–30 nm) were also deposited by RF sputter deposition at 600 °C and 15 mTorr on 6 mm diameter, 0.5 wt% Nb-doped $SrTiO_3$ (001), (011), and (111) single-crystal substrates. Prior to deposition, the substrates were etched and annealed to produce TiO_2-terminated surfaces.

Electrochemical characterization

Electrochemical measurements were performed using an Autolab PGSTAT 302N potentiostat. Gold or platinum wires and Ag/AgCl were used as counter electrodes and reference electrodes, respectively. The electrolyte (0.1 M KOH or $HClO_4$) was prepared with Millipore deionized water. A typical three electrode, fluorinated ethylene propylene cell was used to avoid contamination. Potentials are reported with respect to that of the reversible hydrogen electrode (RHE).

In situ X-ray electrochemical study

X-ray measurements were performed at Sector 12BM of the Advanced Photon Source, Argonne National Laboratory. The *in situ* X-ray electrochemical cell was designed for use with 6 mm diameter, 0.5 mm thick substrates.

Acknowledgements

This work was supported by the U.S. Department of Energy, Basic Energy Sciences, Materials Sciences and Engineering Division. Use of the Advanced Photon Source and Center for Nanoscale Materials was supported by the U.S. Department of Energy, Office of Science, Office of Basic Energy Sciences, under Contract no. DE-AC02-06CH11357.

References

1 K. Kinoshita, *Electrochemical Oxygen Technology*, John Wiley & Sons, 1992.
2 W. Vielstich, H. Yokokawa, H. A. Gasteiger, *Handbook of Fuel Cells: Fundamentals Technology and Applications. Advances in Electrocatalysis, Materials, Diagnostics and Durability: Part 1*, John Wiley & Sons, 2009.
3 D. Strmcnik, *et al.*, *Nat. Chem.*, 2013, **5**, 300–306.
4 S. Trasatti, *Electrochim. Acta*, 1984, **29**, 1503–1512.
5 S. Trasatti and G. Buzzanca, *J. Electroanal. Chem. Interfacial Electrochem.*, 1971, **29**, A1–A5.
6 J. Greeley and N. M. Markovic, *Energy Environ. Sci.*, 2012, **5**, 9246–9256.
7 J. Rossmeisl, A. Logadottir and J. K. Nørskov, *Chem. Phys.*, 2005, **319**, 178–184.
8 J. O. Bockris and T. Otagawa, *J. Phys. Chem.*, 1983, **87**, 2960–2971.
9 Y. Matsumoto and E. Sato, *Mater. Chem. Phys.*, 1986, **14**, 397–426.
10 S. Ardizzone, G. Fregonara and S. Trasatti, *Electrochim. Acta*, 1990, **35**, 263–267.
11 R. Subbaraman, *et al.*, *Nat. Mater.*, 2012, **11**, 550–557.
12 N. Danilovic, *et al.*, *J. Phys. Chem. Lett.*, 2014, **5**, 2474–2478.
13 S. H. Chang, *et al.*, *Nat. Commun.*, 2014, **5**, 4191.
14 T. Sano, D. M. Saylor and G. S. Rohrer, *J. Am. Ceram. Soc.*, 2003, **86**, 1933–1939.
15 G. Koster, *et al.*, *Rev. Mod. Phys.*, 2012, **84**, 253–298.
16 S. H. Chang, Y. J. Chang, S. Y. Jang, D. W. Jeong, C. U. Jung, Y.-J. Kim, J.-S. Chung and T. W. Noh, *Phys. Rev. B: Condens. Matter Mater. Phys.*, 2011, **84**, 104101.
17 Y. Hikita, Y. Kozuka, T. Susaki, H. Takagi and H. Y. Hwang, *Appl. Phys. Lett.*, 2007, **90**, 143507.